Elastic Stress Domains and the Herringbone Reconstruction on Au(111)

Shobhana Narasimhan

Department of Physics 510A, Brookhaven National Laboratory, Upton, New York 11973

David Vanderbilt

Department of Physics and Astronomy, Rutgers University, Piscataway, New Jersey 08855-0849
(Received 18 March 1992)

We suggest that the herringbone reconstruction of the Au(111) surface results from the spontaneous formation of "stress domains." The surface is described theoretically by a 2D Frenkel-Kontorova model. Upon including long-range elastic interactions, the stress-domain pattern is energetically favored. The surface topography and structure factor obtained by relaxing atomic coordinates using molecular dynamics bear a strong resemblance to scanning tunneling microscopy pictures and x-ray scattering data, respectively. Our numerical estimate for the separation between domain walls is consistent with experimental results.

The reconstruction of the (111) surface of gold is unusual and not yet completely understood. It has been known for some time that the surface layer spontaneously densifies along one of the three $\langle \bar{1}10 \rangle$ directions, resulting in a $(n \times \sqrt{3})$ unit cell ($n \sim 22$) containing $2n + 2$ surface atoms. Presumably, this occurs in response to the strong tensile stress that would be present on the unreconstructed surface [1]. Moreover, recent experiments using x-ray diffraction [2] and scanning tunneling microscopy (STM) [3,4] have revealed the surprising presence of an additional superstructure: There is a regular alternation of domains of two (out of the possible three) orientations of the $(n \times \sqrt{3})$ cell, resulting in a striking herringbonelike pattern, with a domain width of ~ 150 Å. Ordering on such a large length scale suggests the presence of a hitherto neglected long-range interaction. Another reason for interest in the herringbone reconstruction is that it plays a critical role in the growth of metal overlayers such as Ni and Co, which are found to nucleate at the "elbows" of the herringbones [5,6].

The herringbone reconstruction is not favored within the context of previous theoretical descriptions of the Au(111) surface, because of the energy cost of making domain walls. In this paper, we suggest that the inclusion of long-range elastic interactions stabilizes the herringbone pattern, which is comprised of the "stress domains" predicted by the theory of Marchenko [7], and of Alerhand *et al.* [8]. They showed that crystal surfaces that possess an orientational degeneracy of reconstructed phases, and have an anisotropic stress tensor, should spontaneously exhibit a regular tesselation of elastic-stress domains. While the possibility that these stress domains may form on Si(100) has received much attention, they have not yet been observed on Si(100), probably because their formation is preempted by kinetically favored step undulations [9], and also because sample miscut leads to terrace widths that are smaller than the predicted width of a single stress domain. Thus, the herringbone structure may constitute the first direct observation of stress domains in any physical system. The

Au(111) surface satisfies the necessary conditions for the formation of stress domains, since the $(n \times \sqrt{3})$ cell has three possible orientations, and an anisotropic stress tensor (since the incorporation of the extra atoms serves to relieve the tensile stress along the $\langle \bar{1}10 \rangle$ direction, but not in the transverse direction). Under these conditions, it is shown in Refs. [7] and [8] that for large enough domain sizes, the formation of stress domains is *always favored*; it remains for us to check whether this length scale is sufficiently short to account for the observed herringbone structure.

The $(n \times \sqrt{3})$ reconstruction is thought to arise from the competition between two effects: (i) the preferred surface bond length is less than that in the bulk; and (ii) the surface atoms prefer to sit in the minima of the potential due to the substrate atoms, and thus remain in registry with the bulk. This situation can be described by the Frenkel-Kontorova (FK) model [10], where nearest-neighbor atoms are connected by springs, and sit in a substrate potential that contains the effects of the bulk. There are two competing sites for surface atoms: The bulk fcc stacking sequence along the [111] direction can terminate either on an fcc site (. . . *ABCABC* or "*C*" site) or on an hcp site (. . . *ABCABA* or "*A*" site). The latter are local minima of slightly higher energy. By occupying both C (fcc) and A (hcp) sites, the surface bond length can be reduced; alternating domains of fcc-like and hcp-like structures are separated by soliton walls, where atoms occupy the "bridge" sites halfway between the A and C sites. The atoms in these transition regions are packed closer together, and are raised with respect to the surface plane, resulting in the surface corrugation observed by STM; the width of the fcc-like region is larger than that of the hcp-like region since the C sites are lower in energy than the A sites.

Initially, one-dimensional FK models with known solutions were applied to Au(111) [11,12], but it is not clear that the mapping to a 1D system is strictly valid. We choose to follow Takeuchi, Chan, and Ho [13], by using a more realistic two-dimensional substrate potential, which

is expanded as a 2D Fourier series of the form

$$V_S(\mathbf{r}) = \sum_{\mathbf{G}} V_S(\mathbf{G}) e^{-i\mathbf{G}\cdot\mathbf{r}}$$

$$= V_0 + 2 \sum_{\mathbf{G} \in \mathcal{G}_2} [V_R \cos(\mathbf{G}\cdot\mathbf{r}) - V_I \sin(\mathbf{G}\cdot\mathbf{r})]$$

$$+ \sum_{\mathbf{G} \in \mathcal{G}_3} V_2 \cos(\mathbf{G}\cdot\mathbf{r}). \tag{1}$$

Here $\mathcal{G}_2$ is a set of three of the six reciprocal-lattice vectors (RLVs) of length $4\pi/\sqrt{3}a$ (with 120° mutual angles), and $\mathcal{G}_3$ consists of the six RLVs of length $4\pi/a$, where $a = 2.884$ Å is the lattice constant of Au. The values of the coefficients V_0, V_R, V_I, and V_2 are obtained by fitting to the first-principles results of Takeuchi, Chan, and Ho [13] for the value of the V_S when the topmost layer of atoms occupies the A, B, C, and bridge sites. This gives $V_0 = -8.025$ mRy, $V_R = 1.483$ mRy, $V_I = -0.087$ mRy, and $V_2 = -0.146$ mRy.

The surface energy of each $(n \times \sqrt{3})$ cell is then given by the sum of a term due to the substrate potential and a term describing the potential energy of the intralayer bonds:

$$E = \sum_i V_S(\mathbf{r}_i) + \frac{1}{2} \sum_j k(l_j - b)^2. \tag{2}$$

The first term is a sum over all atoms in the $(n \times \sqrt{3})$ cell, whose positions are given by $\mathbf{r}_i$; the second term is a sum over the bonds (springs) that connect each atom to its six nearest neighbors, l_j is the length of the bond j, k is the spring constant of the bonds, and b is their preferred equilibrium length $(b < a)$. The zero of energy in Eq. (2) is arbitrary. In principle, Eq. (2) should also contain a term describing the chemical potential, since we are considering reconstructions where the surface density changes [1]. However, we have found empirically that such a term can be regarded, to a first approximation, as having been absorbed into our choice of the preferred surface bond length b [14].

The equilibrium configuration is determined by performing a molecular-dynamics simulation using the method of steepest descent; we verified that we had indeed found the true ground state by checking that a wide variety of initial states all relaxed to the same final state. The value of b and k are chosen such that the surface energy density is minimized at $n = 22$, and to reproduce the experimentally observed value of 0.5 for the relative width of the hcp-like and fcc-like regions [15]. We thus obtain $b = 2.7744$ Å and $k = 90$ mRy/Å^2. We find that the transition from C to A sites is gradual rather than sharp, which agrees with some previous results [13]. However, it is convenient to retain a description in terms of soliton walls separating hcp and fcc domains, even though these features are not sharply defined. [To avoid potential confusion, we point out that the terminology used in this paper is such that *soliton walls* separate hcp-like and fcc-like regions within the $(n \times \sqrt{3})$ reconstruction, whereas *domain walls* separate different orientations of the $(n \times \sqrt{3})$ reconstruction.] We find that the maximum transverse displacement (along $[11\bar{2}]$) is 0.88 Å; this may be compared with experimental values of 0.7 ± 0.3 Å [15] and 0.9 Å [4].

We now apply these same techniques to study the herringbone pattern, which is depicted schematically in Fig. 1. The soliton walls form zigzag lines that bend by 120° at the domain walls, which run parallel to the y axis and are separated by a distance l. The bonding topology is such that alternate soliton walls contain dislocations at every "elbow" where the walls bend. Each dislocation consists of a pair of atoms, one of which has 5 (instead of 6) bonds connecting it to nearest neighbors, while the other atom has a bond coordination of 7. The remaining soliton walls are free of such dislocations; sixfold bond coordination is maintained throughout. Following the authors of Ref. [5], we will refer to these two kinds of soliton walls (with and without point dislocations) as being of type x and type y, respectively.

We have confirmed that, in the absence of terms describing long-range elastic interactions, the surface energy density of the herringbone pattern is always greater than that of the $(n \times \sqrt{3})$ cell, due to the positive energy contribution from the domain walls [since the energetically favorable $(n \times \sqrt{3})$ reconstruction is disrupted in the neighborhood of the walls]. Upon computing this additional energy term when l is large, we find that the energy per unit length of each domain wall is $C_1 = 6.6 \pm 0.2$ meV/Å.

We now include substrate-mediated long-range elastic interactions, following the treatment of Ref. [8], and obtain a theoretical estimate of the domain wall separation l, to check whether it is plausible that this elastic mechanism is in fact responsible for the observed superstructure. The equilibrium value of l is determined by balancing the domain wall energy against the elastic relaxation energy term which favors a reduction in the anisotropy of
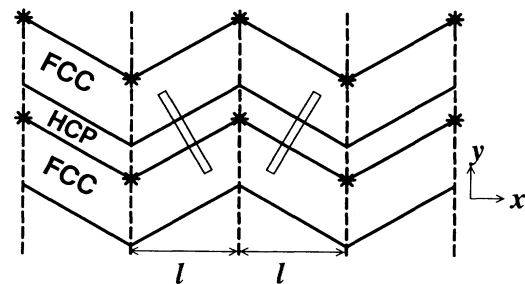

FIG. 1. Schematic depiction of the herringbone reconstruction. The x axis is along $[1\bar{1}0]$, and the y axis along $[\bar{1}\bar{1}2]$. Domain walls run parallel to the y axis and are indicated by heavy dashed lines; soliton walls are represented by heavy solid lines that separate regions of fcc-like and hcp-like stacking. Stars show the positions of point dislocations. Light solid lines outline $(n \times \sqrt{3})$ subunits, which have alternating orientations in alternate domains.

the surface stress tensor. The latter term is given, within continuum elastic theory, by the sum in reciprocal space [8]:

$$E_{el} = -\tfrac{1}{2}\sum_{G_x}|f_y(G_x)|^2\chi_{yy}(G_x) \, , \qquad (3)$$

where χ_{yy} is the elastic Green's function that relates displacements along $\hat{y}$ in the surface layer to the force density f_y. For the geometry depicted in Fig. 1, the force density is given by

$$f_y(x,y) = \pm\frac{\sqrt{3}}{2}(\sigma_\| - \sigma_\perp)\delta(x - x_0) \, , \qquad (4)$$

where $\{x_0\}$ denotes the positions of the domain walls, and $\sigma_\|$ and $\sigma_\perp$ are the components, along the "n" and "$\sqrt{3}$" directions, respectively, of the surface stress tensor for the $(n\times\sqrt{3})$ reconstruction. $\chi_{yy}(G_x)$ has the form $1/\mu G_x$, where μ is a shear modulus. For the type of shear strains appropriate to our problem, we must take $\mu = (c_{11} - c_{12} + 4c_{44})/6$. Upon using experimental values for the elastic constants [16], we obtain $\mu = 203$ meV/Å^3. The elastic relaxation energy can now be rewritten in the form [8]

$$E_{el} = -\frac{C_2}{l}\ln\left[\frac{l}{\pi a_d}\right] \, , \qquad (5)$$

where

$$C_2 = \frac{3}{8\pi}\frac{(\sigma_\perp - \sigma_\|)^2}{\mu} \, . \qquad (6)$$

Here a_d represents the length scale over which the force density at the domain walls falls off to zero, i.e., a_d is the width of a domain wall. The surface energy density is minimized when the separation between domain walls is given by [8]

$$l_0 = \pi a_d e^{C_1/C_2 + 1} \, . \qquad (7)$$

To obtain the domain wall width a_d we examine the variation of some quantity that is finite at the domain walls but zero for a pure $(n\times\sqrt{3})$ reconstruction. Such a quantity is obtained by first computing f_S, the force due to the substrate potential, at relaxed atomic coordinates, and then seeing how $\mathcal{F}$, the difference in f_S at the sites of corresponding atoms in neighboring $(n\times\sqrt{3})$ cells, varies through the unit cell of the herringbone pattern. Figure 2 shows two examples of how $\mathcal{F}$ varies as a function of the x coordinate, suggesting that a suitable value of a_d lies somewhere between $3a$ and $8a$.

Regarding the surface stress anisotropy $\sigma_\perp - \sigma_\|$, we are unfortunately not aware of any first-principles calculations of the surface stress tensor for the $(n\times\sqrt{3})$ structure. Such a calculation has been performed for the unreconstructed (1×1) structure by Needs and Mansfield [1], who obtain a value of 173 meV/Å^2 for the surface stress g. If the $(n\times\sqrt{3})$ structure could be assumed to relieve the stress entirely in the n direction, but not at all in the $\sqrt{3}$ direction, this would lead to $\sigma_\perp - \sigma_\| = 173$
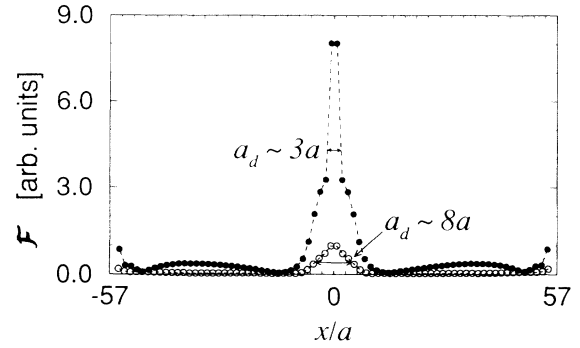

FIG. 2. Plots showing how $\mathcal{F}$, the magnitude of the difference in f_S between neighboring atoms, varies along a row of atoms (i) along a soliton wall (solid circles), and (ii) in the middle of an fcc-like region (open circles), for $n = 21$ and $l = 57a$. There are domain walls at $x/a = -57,0,57$.

meV/Å^2. However, this is undoubtedly an overestimate. The FK model used above yields ratios $\sigma_\|(n\times\sqrt{3})/\sigma(1\times1) = 0.16$ and $\sigma_\perp(n\times\sqrt{3})/\sigma(1\times1) = 0.77$. While this model may not be reliable for estimating absolute surface stresses [17], these *ratios* appear quite reasonable. With these considerations in mind, we take as our best estimate $\sigma_\perp - \sigma_\| = 105 \pm 20$ meV/Å^2 for the stress anisotropy in the $(n\times\sqrt{3})$ cell.

Upon substituting our values for a_d, C_1, and $\sigma_\perp - \sigma_\|$ into Eqs. (6) and (7), we obtain the result that the predicted domain wall spacing l_0 lies between 140 and 980 Å. Some of the experimentally reported values of l (at room temperature) are 162 Å [2], 140 Å [4], 125 Å, and 150 Å [6]; we therefore feel that our calculation provides strong evidence that long-range elastic interactions are responsible for the herringbone reconstruction. A more precise estimate of l_0 could be obtained by calculating the surface stress tensor for the $(n\times\sqrt{3})$ cell more precisely, evaluating the dislocation core energy more accurately (e.g., by including bond strength effects around the fivefold and sevenfold coordinated atoms), and perhaps also going beyond the approximation of a continuous elastic medium. However, the very large size of the unit cell makes more exact calculations difficult.

We find that the relaxed surface configuration obtained from the FK model agrees well with both x-ray and STM experiments. It has been verified [18] that the structure factor for the herringbone cell, computed using our relaxed coordinates, is in accordance with that deduced from x-ray scattering. In Fig. 3, we show what the relaxed structure looks like for $l = 147$ Å. Each atom has been shaded according to the value of the substrate potential at its relaxed coordinates; lighter atoms denote a higher value of the substrate potential. Such a shading scheme should essentially reproduce the surface corrugation observed by STM. A comparison of Fig. 3 with STM pictures [3–6] reveals a striking similarity of features. The light ridges in the figure correspond to soli-
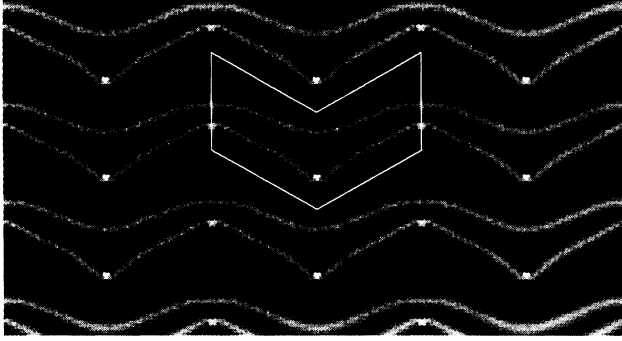
FIG. 3. Picture of the herringbone reconstruction, for $n = 21$ and $l = 147$ Å. The boundary of a unit cell is indicated. Each atom is shaded according to the value of V_S at its relaxed coordinate; lighter atoms sit at higher values of V_S. This figure essentially reproduces the surface structure as seen by STM.

ton walls where atoms sit in bridge sites and are raised relative to the surface plane. Broad dark bands correspond to fcc-like regions, and narrow dark bands correspond to hcp-like regions. There is a clearly observable difference between soliton walls of types x and y. The former have pointed elbows, whereas the latter have more rounded elbows. As a result, alternate domain walls have either very narrow, pinched-off hcp-like regions or broad hcp regions that are equal in width to the fcc regions. A close examination of Fig. 3 reveals a very high contrast in the shading of neighboring atoms at the sites of the dislocations; this agrees with a reported STM observation [4] that the corrugation amplitude of the reconstruction is increased near elbows at domain boundaries.

In summary, we have applied the theory of stress domains to the Au(111) surface, which we have described using a combination of a 2D Frenkel-Kontorova model and continuum elasticity theory. We find that for the herringbone pattern to be favored, it is necessary to include long-range elastic interactions mediated by the substrate. Our theoretical estimate for the domain wall spacing l is consistent with experimentally measured values. Thus, we provide an answer to the puzzle of what causes the herringbone reconstruction, and also confirm that long-range elastic interactions do indeed lead to interesting phenomena at mesoscopic length scales.

[1] R. J. Needs and M. Mansfield, J. Phys. Condens. Matter 1, 7555 (1989).
[2] K. G. Huang, D. Gibbs, D. M. Zehner, A. R. Sandy, and S. G. J. Mochrie, Phys. Rev. Lett. 65, 3313 (1990); A. R. Sandy, S. G. J. Mochrie, D. M. Zehner, K. G. Huang, and D. Gibbs, Phys. Rev. B 43, 4667 (1991).
[3] D. D. Chambliss and R. J. Wilson (to be published).
[4] J. V. Barth, H. Brune, G. Ertl, and R. J. Behm, Phys. Rev. B 42, 9307 (1990).
[5] D. D. Chambliss, R. J. Wilson, and S. Chiang, Phys. Rev. Lett. 66, 1721 (1991).
[6] B. Voigtländer, G. Meyer, and N. M. Amer, Phys. Rev. B 44, 10354 (1991).
[7] V. I. Marchenko, Pis'ma Zh. Eksp. Teor. Fiz. 33, 397 (1981) [JETP Lett. 33, 381 (1981)].
[8] O. L. Alerhand, D. Vanderbilt, R. D. Meade, and J. D. Joannopoulos, Phys. Rev. Lett. 61, 1973 (1988).
[9] J. Tersoff and E. Pehlke, Phys. Rev. Lett. 68, 816 (1992).
[10] Y. I. Frenkel and T. Kontorova, Zh. Eksp. Teor. Fiz. 8, 1340 (1938); F. C. Frank and J. H. van der Merwe, Proc. R. Soc. London 198, 205 (1948).
[11] M. El-Batanouny, S. Burdick, K. M. Martini, and P. Stancioff, Phys. Rev. Lett. 58, 2762 (1987); R. Ravelo and M. El-Batanouny, Phys. Rev. B 40, 9574 (1989).
[12] M. Mansfield and R. J. Needs, J. Phys. Condens. Matter 2, 2361 (1990).
[13] N. Takeuchi, C. T. Chan, and K. M. Ho, Phys. Rev. B 43, 13899 (1991).
[14] We have verified, using test values of the chemical potential, and the correspondingly shifted values of b required to reproduce the correct periodicity, that the final relaxed configurations [for both the $(n \times \sqrt{3})$ and herringbone] are essentially indistinguishable from those obtained with the chemical potential set to zero.
[15] Ch. Wöll, S. Chiang, R. J. Wilson, and P. H. Hippel, Phys. Rev. B 39, 7988 (1989).
[16] J. Delaunay, in Solid State Physics, edited by H. Ehrenreich and D. Turnbull (Academic, New York, 1956), Vol. 2, p. 220.
[17] In the FK model, there is an undetermined contribution to the surface stress coming from the variation of the substrate potential with strain. In fact, the magnitude of the stress of the (1×1) surface is underestimated relative to that of Needs and Mansfield by a factor of ~ 2.1. However, we also note that their calculation does not permit relaxation of interlayer separations perpendicular to the surface, resulting in an overestimate of g.
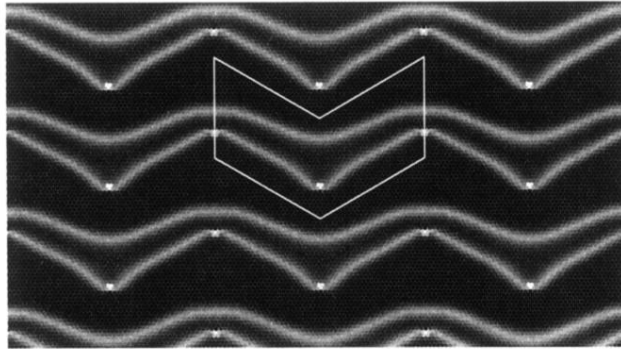[18] A. R. Sandy, Ph.D. thesis, MIT, 1991 (unpublished).

FIG. 3. Picture of the herringbone reconstruction, for $n=21$ and $l=147$ Å. The boundary of a unit cell is indicated. Each atom is shaded according to the value of V_S at its relaxed coordinate; lighter atoms sit at higher values of V_S. This figure essentially reproduces the surface structure as seen by STM.